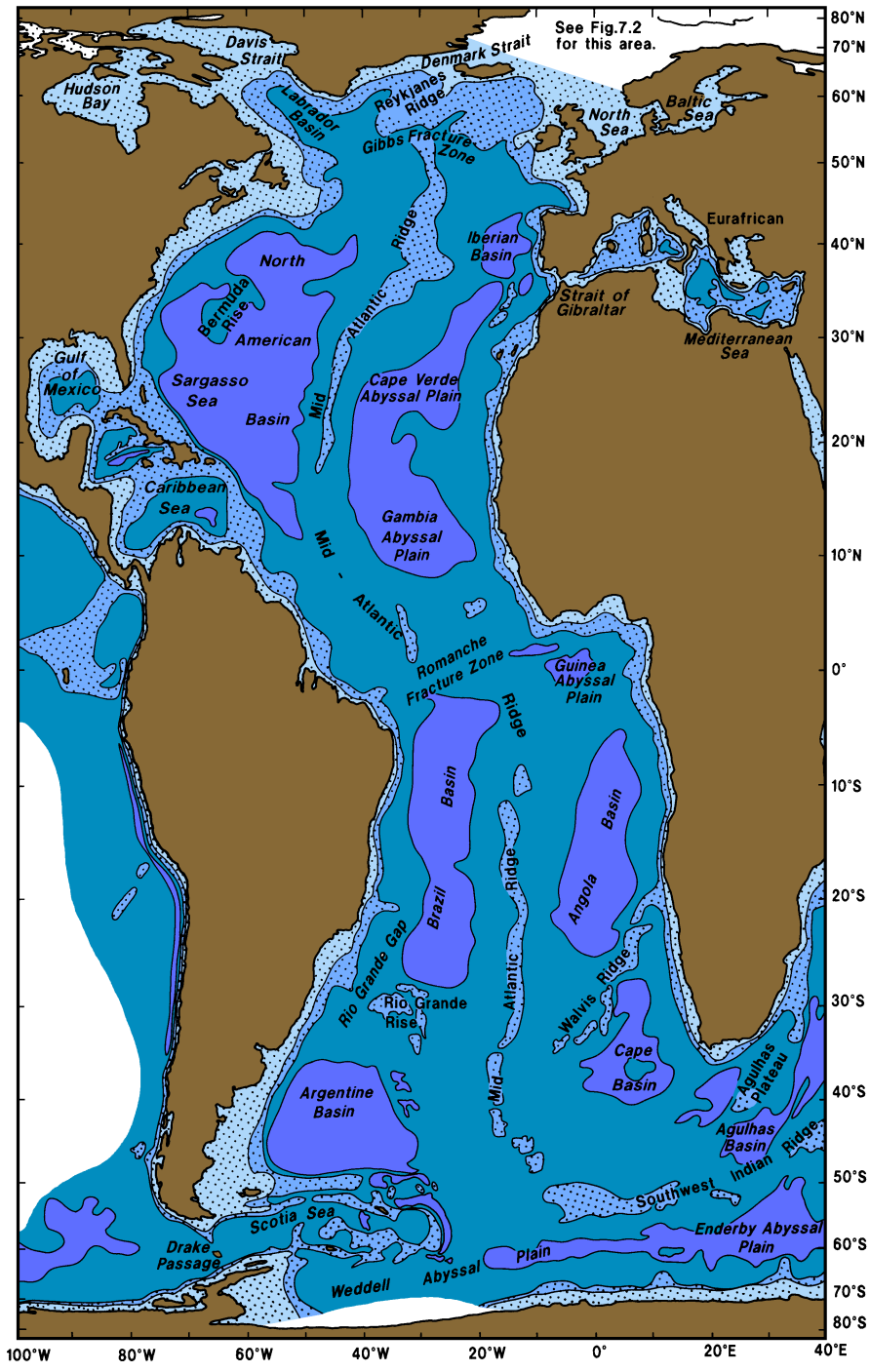

Fig. 14.1. Topography of the Atlantic Ocean. The 1000, 3000, and 5000 m isobaths are shown, and regions less than 3000 m deep are shaded.

rather like the North Pacific ITCZ but not as accurately zonal; its annual mean position angles from the equator off Brazil to about 7°N off Sierra Leone.

North of the ITCZ the mean wind stress distribution more closely resembles that of the North Pacific Ocean, though the Atlantic Northeast Trades are not quite as strong in comparison. Their maximum strength is at about 15°N. The North Atlantic Westerlies enter the ocean from the northwest, similar to the North Pacific Westerlies. They bring cold, dry air out over the Gulf Stream, just as the Pacific winds bring cold dry air from Siberia out over the Kuroshio. As their Pacific counterpart, the Atlantic Westerlies veer round to a definite southwesterly direction in the eastern Atlantic Ocean, and the axis of maximum westerly strength is also oriented along a line running east-north-east. The polar Easterlies of the Arctic region are more vigorous in the Atlantic than in any other ocean.

The integrated flow

When the Sverdrup balance was introduced and tested in Chapter 4 we noted that the largest discrepancies between the integrated flow fields deduced from wind stress and CTD data are found in the Atlantic Ocean. We now go back to Figure 4.4 and Figures 4.5 or 4.6 for a more detailed comparison, keeping in mind that with the exception of the Southern Ocean, the CTD-derived flow pattern should describe the actual situation quite well. The largest discrepancy between the two flow fields occurs south of 34°S; it was discussed in Chapters 4 and 11. North of 34°S, the subtropical gyres of both hemispheres are well reproduced from both atmospheric and oceanic data, as in the other oceans. To be more specific, the gradient of depth-integrated steric height across the North and South Equatorial Currents is calculated fairly well from both data sets, and the gradient across the equator in the Atlantic seen in the CTD-derived pattern (one contour crosses the equator; P increases westward, as in the Pacific Ocean) also occurs in the wind-calculated pattern (even though no contour happens to cross the equator in this case). That this must be so is evident by inspection of Figure 1.2 which shows weak mean westerly winds along the equator in the Atlantic Ocean; hence the only term on the right hand side of eqn (4.7) at the equator is negative, and P must increase towards the west. However, the agreement between Figures 4.4 and 4.5 or 4.6 is not as good in the Atlantic as in the other oceans. The major reason for this is the recirculation of North Atlantic Deep Water, which was mentioned already in Chapter 7 and will be further discussed Chapter 15. It makes the assumption of a depth of no motion less acceptable than in the other oceans. The transport of thermocline water from the Indian into the Atlantic Ocean which is part of the North Atlantic Deep Water recirculation is also not included in the flow pattern derived from wind data.

In the region where the two circulation patterns compare well, the Sverdrup relation reveals the existence of strong subtropical gyres in both hemispheres and a weaker subpolar gyre in the northern hemisphere. The gyre boundaries coincide reasonably well with the contour of zero curl($\boldsymbol{t}/f$) (Figure 4.3). The northern subtropical gyre consists (Figure 14.2) of the North Equatorial Current with its centre near 15°N, the Antilles Current east of, and the Caribbean Current through the American Mediterranean Sea, the Florida Current, the Gulf Stream, the Azores Current, and the Portugal and Canary Currents. The southern gyre is made up of the South Equatorial Current which is centred in the southern hemisphere but extends just across the equator, the Brazil Current, the South Atlantic Current, and the

Benguela Current. The subpolar gyre of the northern hemisphere is modified by interaction with the Arctic circulation, to the extent that it is hardly recognizable as a gyre. It involves the North Atlantic Current, the Irminger Current, the East and West Greenland Currents, and the Labrador Current, with substantial water exchange with the Arctic Mediterranean Sea through the North Atlantic Current (and its extension into the Norwegian Current) and the East Greenland Current.

The Sverdrup relation performs particularly well near the equator, where geostrophic gradients are very small. It reveals the existence of an equatorial countercurrent between the North and South Equatorial Currents. As in the Pacific Ocean, this countercurrent flows down the Doldrums; but it is broader and less intense. This results from the reduced width of the Atlantic Ocean and from the fact that the Doldrums (or ITCZ) are not strictly zonal but angle across from Brazil to Sierra Leone, as mentioned earlier.

A notable discrepancy between Figures 4.4 and 4.5 or 4.6 is the failure of the wind-calculated pattern to reproduce the intense crowding of the contours of depth-integrated steric height off North America near Cape Hatteras (35°N). A similar failure occurs in the north-east Pacific Ocean, but it is not as severe there; in the Atlantic Ocean, the wind-calculated flow follows the coast to Labrador (50°N) before flowing east, whereas it in fact breaks away from the coast at Cape Hatteras (as indicated in the CTD-based flow field) and takes on the character of an intense jet.

The equatorial current system

As in the Pacific Ocean, the equatorial current system displays a banded structure when investigated in detail. Figure 14.3 is a schematic summary of all its elements as they occur in mid-year. The *Equatorial Undercurrent* (EUC) is the strongest, with maximum speeds exceeding 1.2 m s^{-1} in its core at about 100 m depth and transports up to 15 Sv. It is driven and maintained by the same mechanism as in the Pacific Ocean (see Chapter 8), strongest in the west and weakening along its path as a result of frictional losses to the surrounding waters. Observations show that it swings back and forth between two extreme positions 90 km either side of the equator at a rate of once every 2 - 3 weeks, while speed and transport oscillate between the maxima given above and their respective minima of 0.6 m s^{-1} and 4 Sv. The EUC was discovered by the early oceanographer John Young Buchanan during the *Challenger* expedition of 1872 - 1876 and described in 1886, but this discovery was forgotten until the discovery of the Pacific EUC in 1952 triggered a search for an analogous current in the Atlantic Ocean. CTD data reveal the presence of the EUC through the vertical spreading of isotherms in the thermocline (Figure 14.4); in the eastern Atlantic Ocean it can be seen as a prominent subsurface salinity maximum.

The three equatorial currents known from the depth-integrated circulation dominate the surface flow (Figure 14.3) and the hydrography (Figure 14.4; see Chapter 8 for a discussion of the relationship between thermocline slope and currents) but appear more complicated in detail. The *North Equatorial Current* (NEC) is a region of broad and uniform westward flow north of 10°N with speeds of 0.1 - 0.3 m s^{-1}. The eastward flowing *North Equatorial Countercurrent* (NECC, the countercurrent seen in the depth-integrated flow field) has similar speeds; it is highly seasonal and nearly disappears in February when the Trades in the northern hemisphere are strongest (Figure 14.5). The *South Equatorial Current*

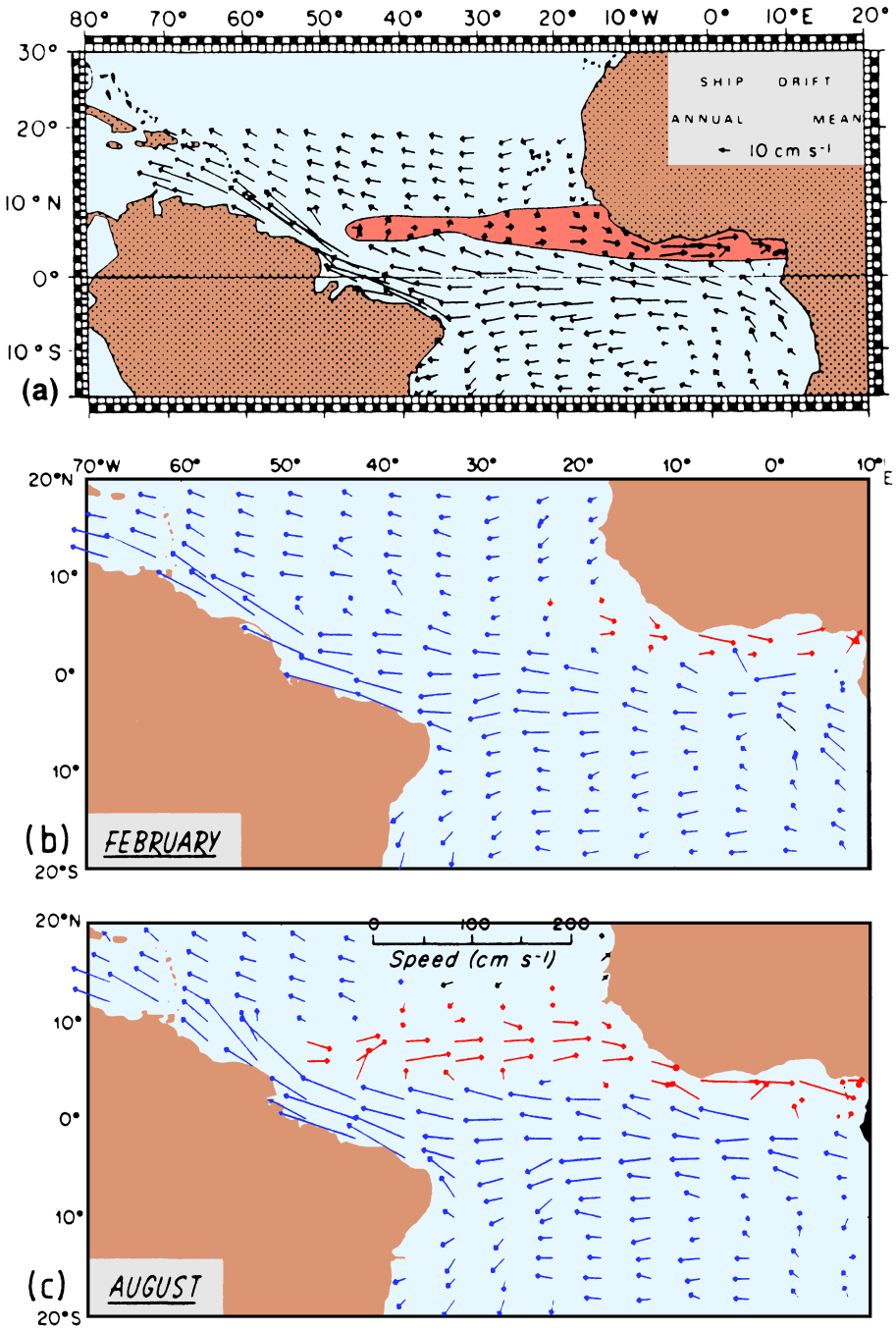

Fig. 14.5. Surface currents in the equatorial region as derived from ship drift data. (a) Annual mean, (b) February, (c) August. From Arnault (1987) and Richardson and Walsh (1986).

Equatorial Undercurrent. We know from our Rules 1, 1a, and 2 of Chapter 3 that cyclonic flow is accompanied by a sea surface depression and an elevation of the thermocline in the centre of the gyre (compare Figure 2.7, or Figures 3.3 and 3.4 which show the same rules operating in an anticyclonic gyre), so in a plot of temperature at constant depth the two gyres should show up as local temperature minima. Figure 14.6 proves that this is indeed the case but only in summer when the Trades of the respective hemisphere are weakest and the Undercurrents strongest. Because of the observed doming of the thermocline in summer the gyres are known as the *Angola* and *Guinea Domes*. The associated circulation exists throughout the year, although weaker in winter, and reaches to at least 150 m depth.

Western boundary currents

The Sverdrup calculation of Chapter 4 gave integrated volume transports for the Gulf Stream and the Brazil Current of 30 Sv. These numbers are modest in comparison to the results for the Kuroshio (50 Sv) or the Agulhas Current (70 Sv). They can be explained in part as reflecting the weakness of the Atlantic annual mean wind stress and the narrowness of the basin. However, they underestimate the Gulf Stream transport by a large margin. This failure of the Sverdrup calculation is a consequence of the recirculation of North Atlantic Deep Water. The westward intensification of all ocean currents influences the flow of Deep Water, too; so both the southward transport of Deep Water at depth and the northward flow of the recirculation below and above the thermocline are concentrated on the western side of the ocean. This adds some 15 Sv to the Gulf Stream transport in the upper 1500 m and subtracts the same amount from the transport of the Brazil Current. This large difference between the two major currents in the Atlantic Ocean does not come out in the vertically integrated flow (Figure 4.7), which shows complete separation of the oceanic gyres along the American coast near 12°S, 6°N, 18°N, and 50°N and similar transports for both boundary currents. This is true for the *wind-driven* component of the flow (i.e. excluding the Deep Water recirculation which is a result of thermohaline forcing), and it is correct when the flow is integrated over all depth, but it is misleading when taken as representative of the circulation in the upper ocean.

For these reasons, the strongest of the western boundary currents is the *Gulf Stream*, so called because it was originally believed to represent a drainage flow from the Gulf of Mexico. It has now been known for many decades that this is not correct and that the flow through the Strait of Florida stems directly from Yucatan Strait and passes the Gulf to the south. Even this flow constitutes only a portion of the source waters of the Gulf Stream. It turns out that it is better to speak of the Gulf Stream System and its various components, the Florida Current, the Gulf Stream proper, the Gulf Stream Extension, and its continuation as the North Atlantic and Azores Currents.

The *Florida Current* is fed from that part of the North Equatorial Current that passes through Yucatan Strait, with a possible contribution from the North Brazil Current (see below). In Florida Strait this current carries about 30 Sv with speeds in excess of 1.8 m s^{-1}. On average, the current is strongest in March, when it carries 11 Sv more than in November. Its transport is increased along the coast of northern Florida through input from the second path of the North Equatorial Current (the Antilles Current, see below). Recirculation of Gulf Stream water in the Sargasso Sea increases its transport further. By

from the subtropical gyre, to feed the Norwegian Current and eventually contribute to Arctic Bottom Water formation. The *Azores Current* is part of the subtropical gyre; it carries some 15 Sv along 35 - 40°N to feed the Canary Current. The remaining transport does not participate in the ocean-wide subtropical gyre but is returned to the Florida Current and Gulf Stream via the much shorter path of the Sargasso Sea recirculation system.

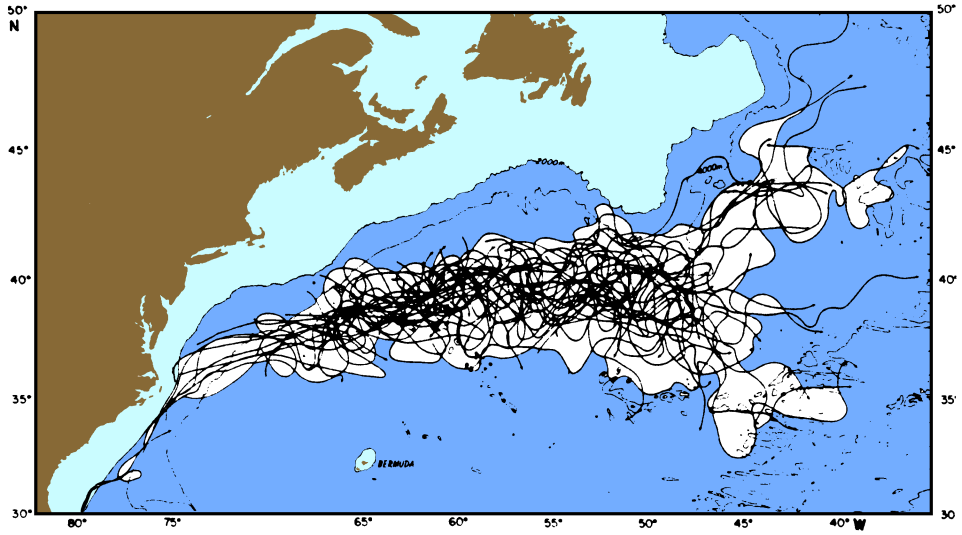

Fig. 14.8. Paths of satellite-tracked buoys in the Gulf Stream system. Most buoy tracks are from the period 1977 - 1981, some tracks going back to 1971. For clarity, only buoys with average velocity exceeding 0.5 m s^{-1} were used and loops indicative of meanders or eddies were removed. The branching of the Gulf Stream into the North Atlantic Current, Azores Current, and Sargasso Sea recirculation is visible in the tracks east of 55°W. From Richardson (1983a).

Free inertial jets which penetrate into the open ocean become unstable along their path. They form meanders which eventually separate as eddies. Meanders which separate poleward of the jet develop into anticyclonic (warm-core) eddies, those separating equatorward produce cyclonic (cold-core) eddies (Figure 14.9). Because of their hydrographic structure - a ring of Gulf Stream water with velocities comparable to those of the Gulf Stream itself, isolating water of different properties from the surrounding ocean - these eddies are often referred to as rings. Most of the Gulf Stream rings are formed in the Gulf Stream Extension region and move slowly back against the direction of the main current (Figure 14.10). Rings formed north of the Gulf Stream are restricted in their movement and often merge with the main flow after a short journey eastward; but the cold-core eddies to the south dominate the Sargasso Sea recirculation region, where some 10 rings can be found at any particular time. Satellite images of sea surface temperature such as Figure 14.11 display them as isolated regions of warm water north of the Gulf Stream and regions of cold water to the south. In the world map of eddy energy (Figure 4.8) the Sargasso Sea recirculation region stands out as one of the most energetic.

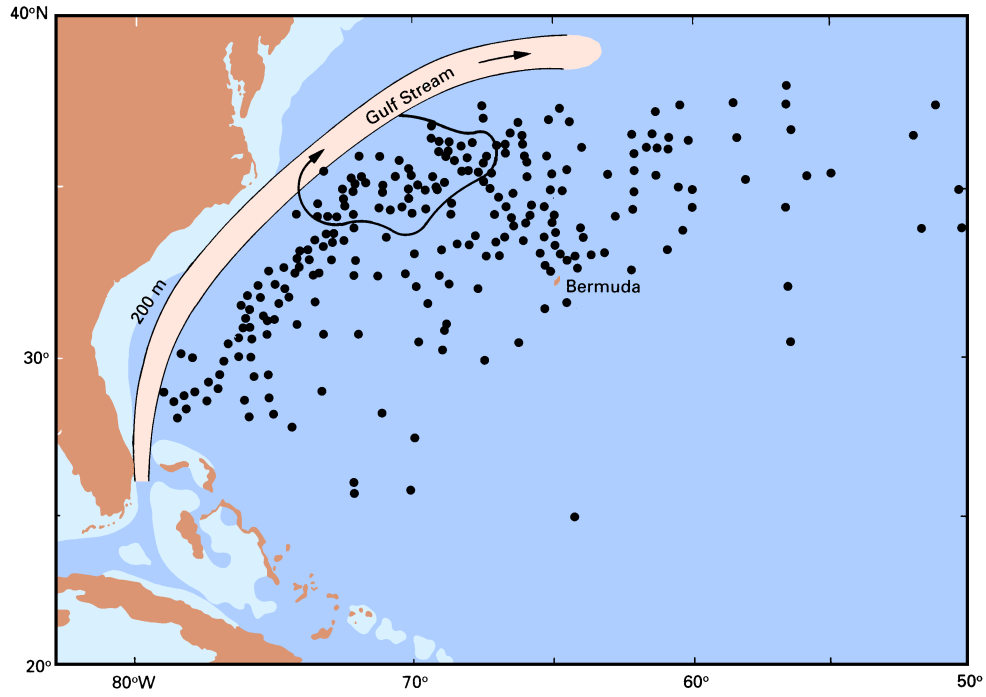

Fig. 14.10. Geographical distribution of 225 cold-core rings reported for the period 1932 - 1983. Ring movement is generally towards the southwest until the rings decay or are absorbed again into the Gulf Stream. The arrow, the path of a ring observed in 1977, gives an example of typical ring movement. Adapted from Richardson (1983b).

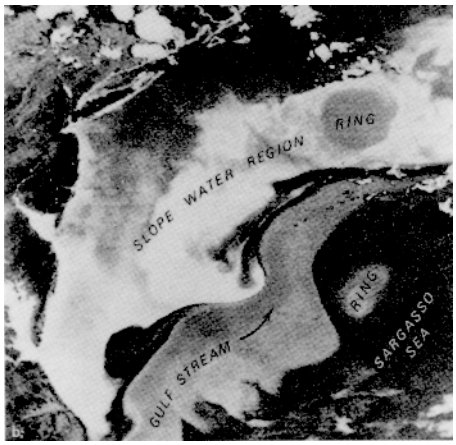

Fig. 14.11. Infrared satellite image of the Gulf Stream System. The Gulf Stream is seen as a band of warm water between the colder Slope Water region and the warmer Sargasso Sea. Two rings can be seen; both contain water of Gulf Stream temperature, but the northern ring is of the warm-core type and has anti-cyclonic rotation, while the ring in the south is a cold-core ring with cyclonic rotation. The region shown covers approximately

dry continental air from the west, exceeds 200 W m^{-2} (Figure 1.6). A brief period of net heat gain occurs from late May to August when warm saturated air is advected from the south (Figure 1.2).

The *Labrador Current* is the western boundary current of the subpolar gyre. This gyre receives considerable input of Arctic water from the East Greenland Current. Measurements south of Cape Farewell indicate speeds of 0.3 m s^{-1} on the shelf and above the ocean floor at depths of 2000 - 3000 m and 0.15 m s^{-1} at the surface, for the combined flow of the East Greenland and Irminger Currents. Transport estimates for the Irminger Current amount to 8 - 11 Sv. Even if this is combined with the estimated 5 Sv for the East Greenland Current of Chapter 7, it does not explain the 34 Sv derived by Thompson *et al*. (1986) for the West Greenland and Labrador Currents from hydrographic section data. Substantial recirculation must therefore occur in the Labrador Sea if these estimates are correct. Earlier estimates of 10 Sv or less were based on geostrophic calculations with 1500 m reference depth, clearly not deep enough for western boundary currents which extend to the ocean floor. The Labrador Current is strongest in February when on average it carries 6 Sv more water than in August. It is also more variable in winter, with a standard deviation of 9 Sv in February but only 1 Sv in August.

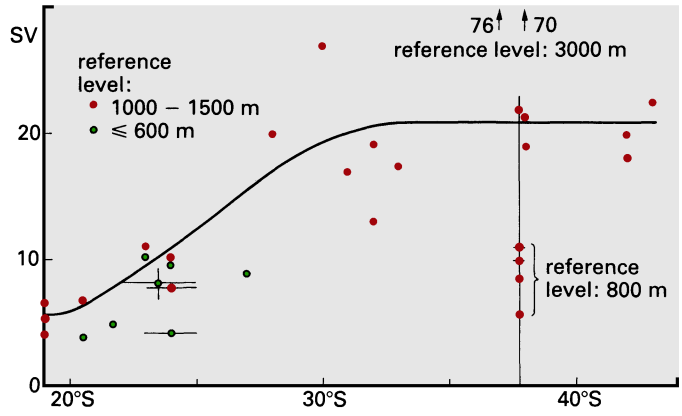

Fig. 14.13. A summary of Brazil Current transports reported in the literature. Unless indicated otherwise, transports assume a level of no motion between 1000 m and 1500 m. After Peterson and Stramma (1991).

The western boundary current of the south Atlantic subtropical gyre, the *Brazil Current*, begins near 10°S with a trickle of 4 Sv supplied by the South Equatorial Current. Over the next 1500 km its strength increases to little more than 10 Sv through incorporation of water from the recirculation region over the Brazil Basin. The current is comparatively shallow, nearly half of the flow occurring on the shelf with the current axis above the 200 m isobath. In deeper water northward flow of Antarctic Intermediate Water is embedded in the Current at intermediate depths (below 400 m). A well-defined recirculation cell south of the Rio Grande Rise (the analogy to the Sargasso Sea recirculation regime of the Gulf Stream) leads to an increase in transport to 19 - 22 Sv near 38°S (Figure 14.13), which

Atlantic and Circumpolar Currents are clearly different regimes. Geostrophic determinations of zonal transport east of 10°W between 30°S (the centre of the subtropical gyre) and 60°S invariably indicate a transport minimum near 45°S, indicating a separation zone between the South Atlantic and Circumpolar Currents. Fig. 14.15. Infrared satellite images of the Brazil Current separation obtained in October 1975 (left) and January 1976 (right). Dark is warm, light is cold; numbers show temperatures in °C. A recently formed eddy with a temperature of 18°C is seen in January 1976 south of the Brazil Current. From Legeckis and Gordon (1982).

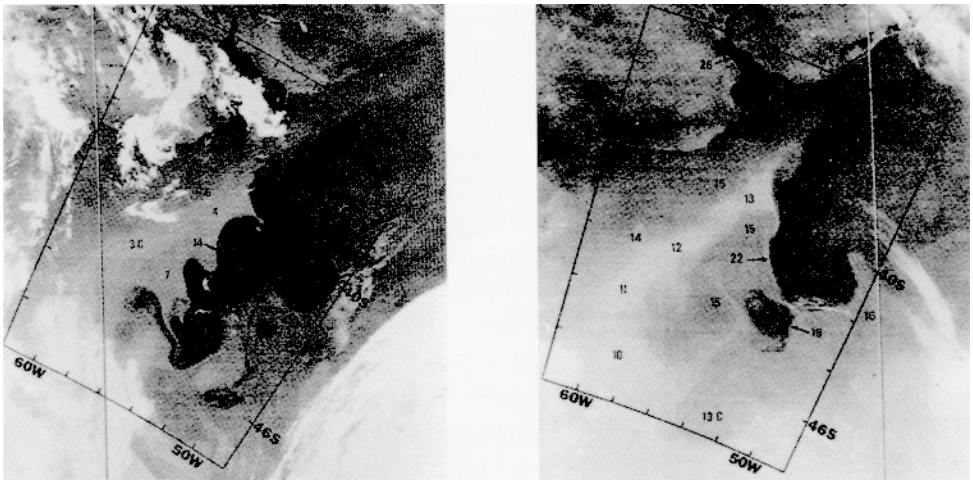

Fig. 14.15. Infrared satellite images of the Brazil Current separation obtained in October 1975 (left) and January 1976 (right). Dark is warm, light is cold; numbers show temperatures in °C. A recently formed eddy with a temperature of 18°C is seen in January 1976 south of the Brazil Current. From Legeckis and Gordon (1982).

Before concluding this section we mention the *North Brazil Current* and *Guyana Current* as another western boundary current system of the Atlantic Ocean. From the point of view of North Atlantic Deep Water recirculation it would be pleasing to see both as elements of continuous northward flow in and above the thermocline which starts at 16°S in the South Equatorial Current and continues through the American Mediterranean Sea to 27°N, eventually feeding into the Florida Current. Although this current system has received much less attention than is warranted by its important role in the global transport of heat, it is fair to say that the continuity of northward flow at the surface is questionable. There is no doubt about the existence of the North Brazil Current; observed surface speeds in excess of 0.8 m s^{-1} testify for its character as a jet-like boundary current. The character of the Guyana Current is much more obscure; eddies related to flow instability have been reported, but some researchers doubt whether the Guyana Current exists as a permanent current. There has also been some documentation (Duncan *et al*., 1982) that the Antilles Current is not identifiable as a permanent feature of the circulation and may indeed not exist as a continuous current. Since the flow from the North Equatorial Current has to reach the

relative to 1500 - 2000 m depth is estimated at 20 - 25 Sv. This compares with a maximum of 7 Sv in the jet of the upwelling system (Peterson and Stramma, 1991).

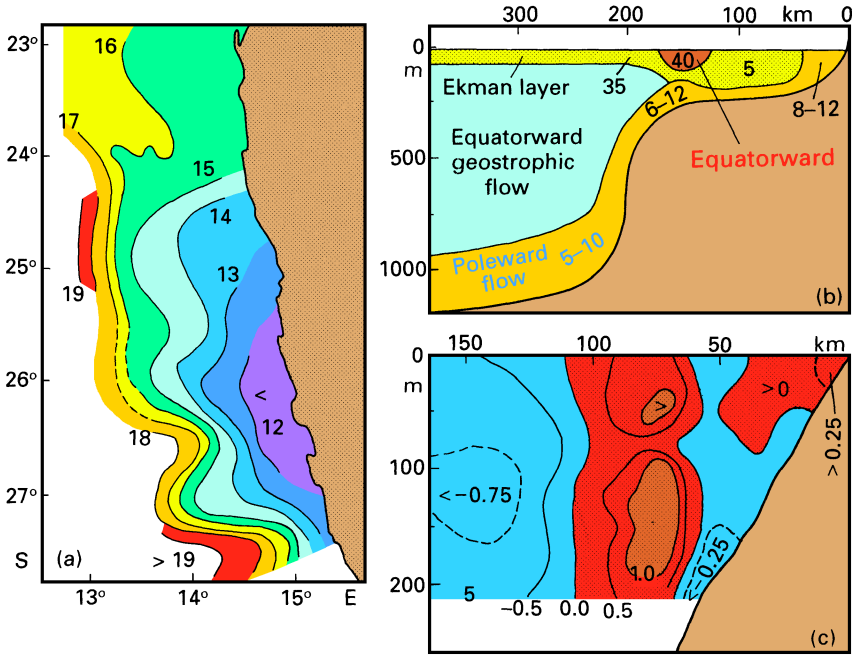

Fig. 14.16. The Benguela Current upwelling system. (a) Sea surface temperature (°C) in the northern part as observed during February 1966. (b) Sketch of the mean circulation. Transverse flow occurs in the bottom and Ekman layers; average speeds are given in cm s^{-1}, westward flow is shaded. Major alongshore (poleward or equatorward) flows are also indicated. (c) Observations of the equatorward jet (m s^{-1}, northward flow is shaded) from January 1973 in the south near 34°S. Adapted from Bang (1971), Nelson (1989), and Bang and Andrews (1974).

Strong seasonal variability and large contrast between the waters in the north and south are the main characteristics of the *Canary Current* upwelling system. Although the width of the upwelling region is narrow (less than 100 km), it exceeds the width of the shelf in most places. Observations on the shelf, which on average is only 60 - 80 m deep, show an unusually shallow Ekman layer at the surface with offshore movement extending to about 30 m depth, an intermediate layer of equatorward geostrophic flow, and a bottom layer with onshore flow (Figure 14.17c). An equatorward surface jet occurs just inshore of the shelf edge, while the undercurrent is usually restricted to the continental slope (Figure 14.17b). Velocities in all components of the current system are similar to those reported from the Benguela Current upwelling system.

The Canary Current upwelling reaches its southernmost extent in winter when the Trades are strongest (Figure 14.18). It then extends well past Cap Blanc, the separation point of the Canary Current from the African coast (Figure 14.2).

observations it is evident as a salinity minimum caused by its high content of South Atlantic Central Water (Figure 14.19).

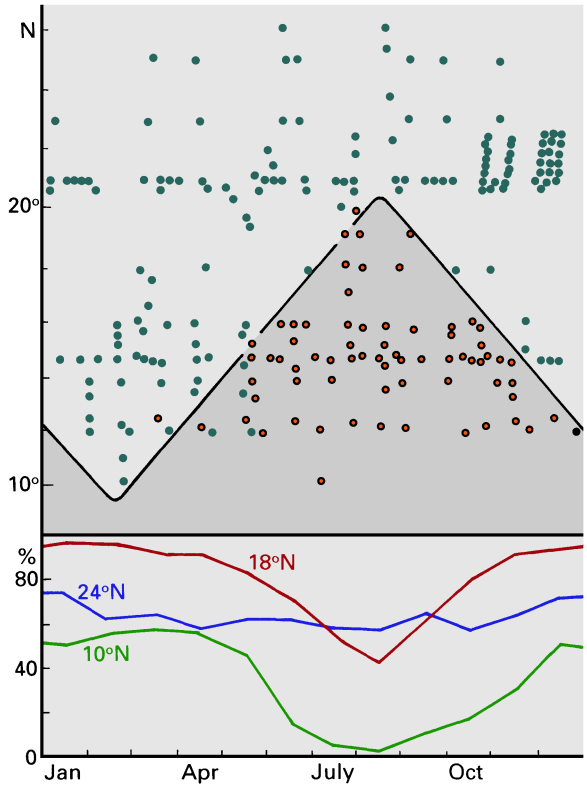

Fig. 14.18. Seasonal variability of the Canary Current upwelling system.

(a) southern boundary of the upwelling region; full dots indicate observed upwelling, circled dots indicate observed absence of upwelling.

(b) frequency of occurrence of winds favorable for upwelling (wind direction is in the quarter between alongshore toward south and exactly offshore). Adapted from Schemainda *et al*. (1975).

A rather unique coastal upwelling region is found along the coasts of Ghana and the Ivory Coast where the African continent forms some 2000 km of zonally oriented coastline. Winds in this region are always very light and never favorable for upwelling. The sea surface temperature, however, is observed to drop regularly by several degrees, for periods of 14 days during northern summer (Figure 14.20). These temperature variations are coupled with reversals of the currents on the shelf, periodic lifting of the thermocline, and advection of nutrient-rich water towards the coast. The upwelling, which is clearly not related to local wind conditions, is caused by variations in the wind field over the *western* equatorial Atlantic Ocean which produce wave-like disturbances of the thermocline in the equatorial region known as Kelvin waves. Equatorial Kelvin waves are a major component of interannual variations in the circulation of the Pacific Ocean; a detailed discussion of their dynamics is therefore included in Chapter 19. For the purpose of the present discussion it is sufficient to note that they consist of a series of depressions and bulges of the thermocline, move eastward along the equator at about 200 km per day, and when reaching the eastern coastline continue poleward. The progression of the thermocline bulges and depressions is

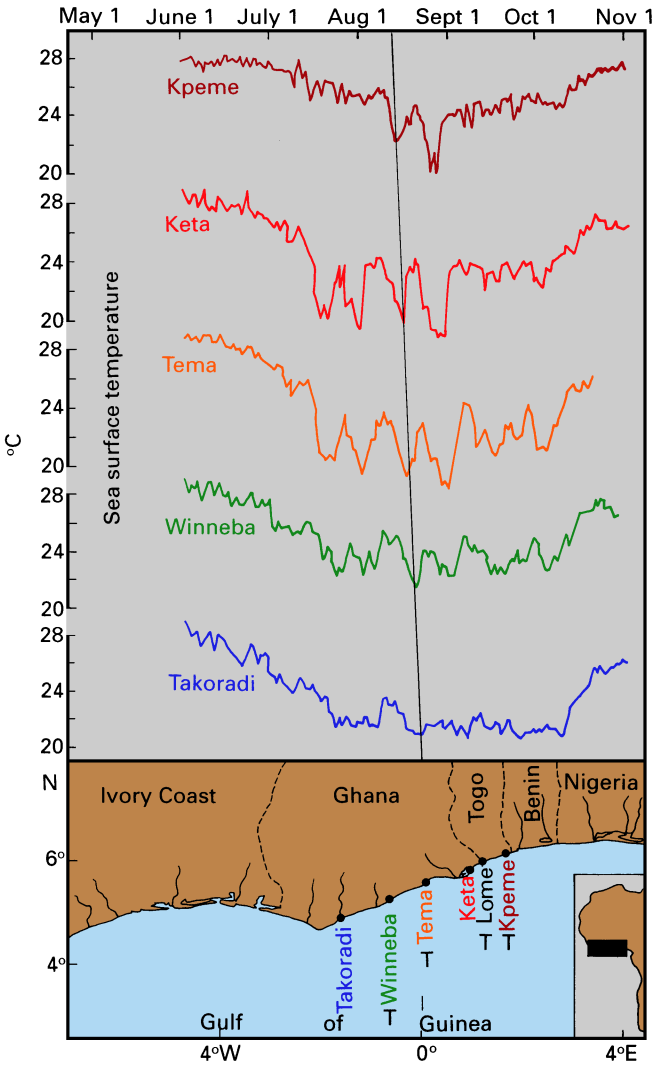

Fig. 14.20. (Right) Sea surface temperature (°C) as observed in 1974 at various locations in the Gulf of Guinea, showing periodic upwelling caused by waves of 14 day period during summer. Note the westward propagation indicated by the tilt of the line through the temperature minima. Adapted from Moore *et al*. (1978).